

# Syntheses, Spectroscopic Properties, Crystal Structures, and Antitumor Activities of the Optically Isomeric Mandelate Chelates, Mandelato(*trans*-1,2-diaminocyclohexane)platinum(II)

T. Ken MIYAMOTO,\* Kojiro OKUDE, Kazuyuki MAEDA, Hikaru ICHIDA, Yuki Yoshi SASAKI, and Tazuko TASHIRO†

Department of Chemistry, Faculty of Science, The University of Tokyo, Hongo, Bunkyo-ku, Tokyo 113

†Cancer Chemotherapy Center, J. C. R., Kami-Ikebukuro, Toshima-ku, Tokyo 170

(Received May 10, 1989)

The four optical isomers of mandelato(*trans*-1,2-diaminocyclohexane)platinum(II) have been prepared. The CD and NMR spectra of these compounds in solution indicate that the mandelate coordinates to platinum(II) to form a five-membered chelate ring. The X-ray crystal structure analyses of a pair of diastereomers, (*R*)-mandelato[(1*R*,2*R*)-1,2-diaminocyclohexane]platinum(II) and (*S*)-mandelato[(1*R*,2*R*)-1,2-diaminocyclohexane]platinum(II), have confirmed that the skeletal configuration of (*R*)- or (*S*)-mandelic acid is retained during the chelation of platinum(II). As a whole, the structural features of both diastereoisomers are analogous to each other. However, slight differences in hydrogen bonding are noticeable in relation to the solubilities. A preliminary animal test against mice leukemia L1210 was carried out using these compounds. The four isomers show different activities. All these facts together support the conclusion that the chiralities of both ammine (carrier) and mandelate (leaving group) influence the antitumor activities of the platinum agents.

Since the discovery of significant antineoplastic activity of *cis*-dichlorodiammineplatinum(II),<sup>1)</sup> this complex has been widely used as an anticancer agent. The drug, however, is highly toxic, especially regarding renal damage. Consequently, a vast number of platinum complexes have been prepared in search of less toxic antitumor agents.

In the process of amelioration, 1,2-diaminocyclohexane (dach) was reported as being a potent ligand (carrier ligand) for antitumor platinum complexes.<sup>2–4)</sup> Kidani et al. resolved three isomers of dach and found that the platinum(II) complexes of each isomer have different antitumor activities against mice leukemia L1210.<sup>5)</sup> The *trans*-dach complexes were more potent than the *cis*-dach complex. The different activities between the *trans*-dach complexes, i.e., (1*R*,2*R*)- and (1*S*,2*S*)-isomeric complexes, were supposed to be derived from chiral recognitions between the active platinum(II) species and their final targets, DNA bases. This point of view leads to one of the most important subjects in drug design: the chirality of the carrier ligand. Further emphasis should be placed on the fact that the anionic ligands (leaving groups) in the platinum complexes also have considerable influence on antitumor activities,<sup>6,7)</sup> and have been supposed to play important roles in drug metabolism. Accordingly, special regard will be paid to not only the chiralities of the carrier ligands, but those of the leaving groups.

Recently, Totani et al. have reported the syntheses of a series of (glycolato-*O,O'*)platinum(II) complexes.<sup>8)</sup> These complexes have a novel chelate ring in which glycolate is bound to platinum(II) with both carboxylato- and alcoholato-oxygens. By using the optically active mandelate(md) as a leaving group instead of glycolate, a chiral point can be brought about in the vicinity of platinum(II).

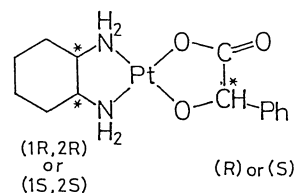


Fig. 1. The proposed structure of [Pt(dach)(md)].

In general, platinum(II) alkoxides are unstable and a limited number of examples are known to date.<sup>9–11)</sup> Therefore, alcoholato-platinum(II) bonding stabilized by chelation arouse interest in the study of the structural characteristics. However, even X-ray crystal structure analysis has not so far been applied to the glycolate or mandelate-chelating complexes.

Thus, we have prepared the four optical isomers of platinum(II) complexes with *trans*-dach and md as ligands; i.e., (*R*)- or (*S*)-mandelato[(1*R*,2*R*)- or (1*S*,2*S*)-1,2-diaminocyclohexane]platinum(II) (Fig. 1). Syntheses, X-ray structure analyses and their properties, including the antineoplastic activities, are described here.

## Experimental

**Materials.** From a commercially available mixture of *trans*- and *cis*-diaminocyclohexane an optically pure (1*R*,2*R*)-*trans*- or (1*S*,2*S*)-*trans*-isomer was resolved according to a method described in the literature.<sup>12)</sup>

The four nitrate complexes, i.e., dinitrato[(1*R*,2*R*)-1,2-diaminocyclohexane]platinum(II); [Pt(*RR*-dach)(NO<sub>3</sub>)<sub>2</sub>], dinitrato[(1*S*,2*S*)-1,2-diaminocyclohexane]platinum(II); [Pt(*SS*-dach)(NO<sub>3</sub>)<sub>2</sub>], *cis*-dinitratodiammineplatinum(II); [Pt(NH<sub>3</sub>)<sub>2</sub>(NO<sub>3</sub>)<sub>2</sub>] and *cis*-dinitratodiisopropylamineplatinum(II); [Pt(*ipr*)<sub>2</sub>(NO<sub>3</sub>)<sub>2</sub>], were prepared using a similar method to that of Lippert et al.<sup>13)</sup>

**The Optical Isomers of Mandelato(*trans*-1,2-diaminocyclohexane)platinum(II):** The compound was synthesized

by the modified method from the literature.<sup>8)</sup> A 4.61 g (11 mmol) portion of [Pt(*RR*-dach)(NO<sub>3</sub>)<sub>2</sub>] was dissolved in 150 ml of water with heating. The solution was passed through a column packed with the anion exchange resin (Diaion SA10AOH, 160 ml) and a further amount of water was passed through the column. To the combined eluate 1.52 g of (*R*)-mandelic acid (10 mmol) was dissolved. After stirring overnight, the solution was evaporated to dryness. A small amount of water was added and the mixture was stirred at 60°C. By filtration, a white powder of (*R*)-mandelato[(1*R*,2*R*)-1,2-diaminocyclohexane]platinum(II) monohydrate [Pt(*RR*-dach)(*R*-md)]·H<sub>2</sub>O was obtained (3.68 g, 8.0 mmol, 80% yield). A crystal suitable for X-ray crystal analysis was obtained by recrystallization from water. In a similar manner, another three optical isomers of mandelato(*trans*-1,2-diaminocyclohexane)platinum(II) were synthesized. Found: [Pt(*RR*-dach)(*R*-md)]·H<sub>2</sub>O: C, 35.16; H, 4.65; N, 5.86%; [Pt(*RR*-dach)(*S*-md)]·H<sub>2</sub>O: C, 35.37; H, 4.62; N, 5.86%; [Pt(*SS*-dach)(*R*-md)]·H<sub>2</sub>O: C, 35.09; H, 4.53; N, 5.81%; [Pt(*SS*-dach)(*S*-md)]·H<sub>2</sub>O: C, 35.23; H, 4.62; N, 5.75%. Calcd for C<sub>14</sub>H<sub>22</sub>N<sub>2</sub>O<sub>4</sub>Pt: C, 35.22; H, 4.62; N, 5.75%.

**(*R*)-Mandelatodiammineplatinum(II) [Pt(NH<sub>3</sub>)<sub>2</sub>(*R*-md)]·1/2H<sub>2</sub>O:** The complex [Pt(NH<sub>3</sub>)<sub>2</sub>(NO<sub>3</sub>)<sub>2</sub>] (1.05 g, 3.0 mmol) was dissolved in water (150 ml) with heating. The solution was passed through a column packed with the anion exchange resin (Diaion SA10AOH, 160 ml) and a further amount of water was passed through the column. To the combined eluate 451 mg of (*R*)-mandelic acid (3.0 mmol) was dissolved. After standing overnight the solution was evaporated to ca. 50 ml. The solution turned pale blue after 3 days of standing. After removing the precipitate the solution was cooled to 0°C overnight. A white crystalline solid containing a small amount of pale blue material was obtained. A blue impurity could not be removed by recrystallization from water. Yield: 23g mg (0.62 mmol, 21%). Found: C, 24.89; H, 3.30; N, 7.21%. Calcd for C<sub>8</sub>H<sub>13</sub>N<sub>2</sub>O<sub>3.5</sub>Pt: C, 24.74; H, 3.37; N, 7.21%.

**(*S*)-Mandelatodiisopropylamineplatinum(II) [Pt(*ipr*)<sub>2</sub>(*S*-md)]:** This complex was similarly synthesized as anhydrous salt: Found: C, 36.25; H, 5.25; N, 5.94%. Calcd for C<sub>14</sub>H<sub>24</sub>N<sub>2</sub>O<sub>3</sub>Pt: C, 36.28; H, 5.22; N, 6.04%.

**Spectroscopy.** The CD spectra were recorded with a JASCO-J500A spectrometer. UV-Vis spectra were obtained by the use of a Hitachi 340 spectrometer.

400-MHz <sup>1</sup>H NMR spectra were measured for [Pt(*RR*-dach)(*R*-md)] and [Pt(*RR*-dach)(*S*-md)] in D<sub>2</sub>O with DSS as an internal standard by the use of a JEOL JNM-GX FT NMR spectrometer. [Pt(*RR*-dach)(*R*-md)]: δ=1.12–1.22 (2H, m, 4- or 5-dach), 1.24–1.33 (2H, m, 4- or 5-dach), 1.55–1.58 (2H, m, 3- or 6-dach), 2.01–2.07 (2H, m, 3- or 6-dach), 2.31–2.35 (2H, m, 1- and 2-dach), 4.931 (1H, s, α-md), 7.39–7.47 (1H, m, *p*-phenyl), 7.44 (2H, d, *J*=8 Hz, *m*-phenyl), 7.65 (2H, d, *J*=8 Hz, *o*-phenyl). [Pt(*RR*-dach)(*S*-md)]: δ=1.12–1.21 (2H, m, 4- or 5-dach), 1.22–1.32 (2H, m, 4- or 5-dach), 1.53–1.61 (2H, m, 3- or 6-dach), 2.00–2.05 (2H, m, 3- or 6-dach), 2.20–2.27 (1H, m, 1- or 2-dach), 2.30–2.37 (1H, m, 1- or 2-dach), 4.93 (1H, s, α-md), 7.37–7.49 (1H, m, *p*-phenyl), 7.45 (2H, d, *J*=7 Hz, *m*-phenyl), 7.72 (2H, d, *J*=7 Hz, *o*-phenyl).

22.5-MHz <sup>13</sup>C NMR spectrum was recorded with a JEOL FX90Q to [Pt(*SS*-dach)(*R*-md)] in DMSO-*d*<sub>6</sub> with TMS as an internal standard. δ=24.2 (2C, 4- and 5-dach), 31.4 (1C, 3- or

6-dach), 31.9 (1C, 3- or 6-dach), 60.9 (1C, 1- or 2-dach), 61.5 (1C, 1- or 2-dach), 79.7 (1C, α-md), 126.3 (2C, *o*-phenyl), 127.3 (3C, *m*-, and *p*-phenyl), 145.5 (1C, 1-phenyl), 189.4 (1C, C=O).

19.2-MHz <sup>195</sup>Pt NMR spectra were measured for [Pt(*RR*-dach)(*R*-md)] (ca. 20 mg cm<sup>-3</sup>) and [Pt(*RR*-dach)(*S*-md)] (ca. 200 mg cm<sup>-3</sup>) in DMSO-*d*<sub>6</sub> with Na<sub>2</sub>PtCl<sub>6</sub> in D<sub>2</sub>O as an external standard. (a JEOL FX90Q) [Pt(*RR*-dach)(*S*-md)]: δ=−1897. [Pt(*RR*-dach)(*R*-md)]: δ=−1904. A new peak (δ=−2968) had been growing for [Pt(*RR*-dach)(*S*-md)] with time, but no change was observed for [Pt(*RR*-dach)(*R*-md)].

The IR spectra were measured with a Hitachi 260-30. ν(C=O)/cm<sup>-1</sup> in KBr disk: [Pt(*RR*-dach)(*R*-md)]·H<sub>2</sub>O: 1649; [Pt(*RR*-dach)(*S*-md)]·H<sub>2</sub>O: 1664; [Pt(NH<sub>3</sub>)<sub>2</sub>(md)]·H<sub>2</sub>O: 1622.

**Solubility Test.** Solubility (mg ml<sup>-1</sup>) in H<sub>2</sub>O (or dmso) at 26°C: [Pt(*RR*-dach)(*R*-md)]·H<sub>2</sub>O: 7.8 (20); [Pt(*RR*-dach)(*S*-md)]·H<sub>2</sub>O: 15.3 (>200).

**X-Ray Diffraction Measurement and Structure Determination.** Among the four optical isomers, a pair of diastereomers, [Pt(*RR*-dach)(*R*-md)]·H<sub>2</sub>O and [Pt(*RR*-dach)(*S*-md)]·H<sub>2</sub>O, were applied to the X-ray crystal structure analysis.

A colorless plate crystal was subjected to an X-ray diffraction measurement. The density of the crystal was measured by a flotation method in mixtures of 1,2-dibromoethane and carbon tetrachloride. X-Ray diffraction intensities were collected on a Rigaku AFC-5R goniometer with graphite monochromatized Mo *K*α (λ=0.71069 Å) radiation (50 kV, 150 mA) at Research Centre for Spectrochemistry, Faculty of Science, The University of Tokyo. The crystal gradually became yellow during exposure to X-rays, but no significant influences was observed regarding the intensities. Data were corrected for both Lorenz and polarization effects. An empirical absorption correction by ψ-scan was applied to both isomers. The positions of the Pt atoms were solved by Mithril,<sup>14)</sup> and other atoms were located by successive Fourier and differential syntheses. An absolute configuration was determined by anomalous scattering factors. The enantiomeric structure was rejected because of the larger *R*-factor. H atoms, except crystal water, were located from calculations, but were not refined. Anisotropic thermal parameters were applied for non-hydrogen atoms and isotropic ones for H atoms. The thermal and positional parameters of all non-hydrogen atoms were refined by full-

Table 1. Crystallographic Data of [Pt(dach)(md)]·H<sub>2</sub>O Isomers

Isomer	<i>RR</i> - <i>R</i>	<i>RR</i> - <i>S</i>
Formula	PtO <sub>4</sub> N <sub>2</sub> C <sub>14</sub> H <sub>22</sub>	PtO <sub>4</sub> N <sub>2</sub> C <sub>14</sub> H <sub>22</sub>
Formula weight	477.43	477.43
Crystal system	Monoclinic	Monoclinic
Space group	<i>P</i> 2 <sub>1</sub>	<i>P</i> 2 <sub>1</sub>
<i>Z</i>	4	4
<i>a</i> /Å	11.778(2)	11.886(1)
<i>b</i> /Å	10.930(2)	10.623(2)
<i>c</i> /Å	12.217(2)	12.104(1)
β/°	90.71(2)	92.98(1)
<i>V</i> /Å <sup>3</sup>	1572.6(9)	1526.3(6)
<i>D</i> <sub>x</sub> /g cm <sup>-3</sup>	2.02	2.08
<i>D</i> <sub>m</sub> /g cm <sup>-3</sup>	1.99	2.06
μ/cm <sup>-1</sup> (Mo <i>K</i> α)	94.05	96.90
<i>F</i> (000)	920	920

Table 2. Measurement Details for [Pt(dach)(md)]·H<sub>2</sub>O Isomers

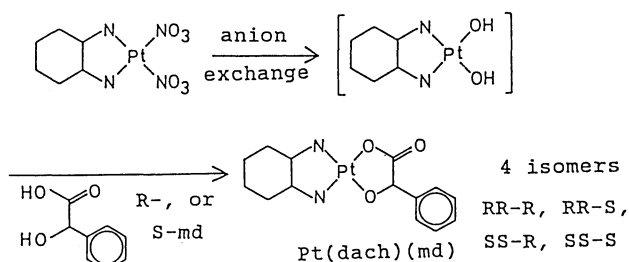
Isomer	<i>RR-R</i>	<i>RR-S</i>
<i>T</i> /K	300	300
No. of measurements	3996	3895
No. of observations	3053	3219
	( $F_o \geq 3.0\sigma(F_o)$ )	( $F_o \geq 3.0\sigma(F_o)$ )
No. of variables	378	378
<i>R</i> ( <i>wR</i> )	0.042(0.039)	0.042(0.052)
<i>S</i>	1.96	1.39
( $\Delta/\sigma$ ) <sub>max</sub>	0.38	0.03
( $\Delta\sigma$ ) <sub>max</sub> /e Å <sup>-3</sup>	2.56	1.54
Crystal dimensions	0.20×0.12×0.05	0.25×0.24×0.15
/mm		
No. of reflections used in cell dimensions ( $\theta$ range/°)	22(19< $\theta$ <20)	24(16< $\theta$ <19)
Mode	$\omega$ -2 $\theta$	$\omega$ -2 $\theta$
Range of measurements (2 $\theta$ /°)	4<2 $\theta$ <55	4<2 $\theta$ <55
Scan rate (° min <sup>-1</sup> in 2 $\theta$ )	6	6
Standard reflections (number/interval)	3/100	3/100
Indices	022, 220, 202	1 -30, -1 -3 1, -3 -1 2
Fluctuation(%)	±5.0	±2.0
<i>h k l</i> range	-18≤ <i>h</i> ≤18 0≤ <i>k</i> ≤17 0≤ <i>l</i> ≤19	0≤ <i>h</i> ≤15 0≤ <i>k</i> ≤14 -16≤ <i>l</i> ≤16
Indices used for $\psi$ scan	-2 0 2, -3 0 3, -3 1 5 -5 0 5, -3 1 8, -6 1 8 -6 1 10	0 2 -2, 0 4 -4, 0 6 -6 0 8 -8, 2 9 -8

matrix least squares on *F* with  $W=1/\sigma(F_o)$ . All calculations were performed with the TEXSAN<sup>15)</sup> program with complex scattering factors from International Tables for X-ray Crystallography<sup>16)</sup> and were carried out on DEC Micro Vax II at the Research Centre for Spectrochemistry. Crystallographic data and measurement details are listed in Tables 1 and 2, respectively. The complete  $F_o-F_c$  data are deposited as Document No. 8893 at the Office of the Editor of Bull. Chem. Soc. Jpn.

**Antitumor Assay in vivo.** The antitumor activities of the [Pt(dach)(md)] isomers against mice leukemia L1210 were tested. 10<sup>5</sup> cells/mouse were transplanted i.p. into CDF<sub>1</sub> mice (6 mice/group) and samples were administered i.p. on days 1, 5, and 9. From the mean survival times of treated (*T*) and control (*C*) mice, *T/C* values were calculated as indicators of activity.

## Results and Discussion

### Syntheses of the Compounds. By the anion



Scheme 1. Synthetic procedure to [Pt(dach)(md)]·H<sub>2</sub>O.

exchange of [Pt(dach)(NO<sub>3</sub>)<sub>2</sub>], dihydroxo species is supposed to be formed in aqueous solution. The dihydroxo complex was neutralized by the addition of the equivalent mandelic acid. The procedure results in the five-membered chelation of platinum(II) (Scheme 1). The neutralization is a relatively slow process: after overnight standing of the reaction mixture at room temperature, an oily product was only obtained; heating of the aqueous solution at 60 °C for several hours gave a crystalline solid. However, at higher temperature (>80 °C), the solution turned red. This coloring indicated a partial decomposition of platinum(II) alkoxide.

In the preparation of [Pt(NH<sub>3</sub>)<sub>2</sub>(md)]·1/2H<sub>2</sub>O without protection to light, the solution turned blue. The addition of excess mandelic acid to this solution precipitated a blue-black solid. The blue product, which showed IR absorption bands due to mandelate and ammine ligands, was assumed a platinum oligomer, such as a "platinum blue"; however, the structure of this compound has not yet been determined. The formation of the oligomeric species by the use of the bidentate ligands seems to be a relatively familiar phenomenon. For example, the well known oligomers of platinum(II) have bidentate bridging ligands such as uracil, pyridone, pyrrolidone, phosphate;<sup>17-19)</sup> in our case mandelate. In the preparation of mandelato-platinum(II) complexes, the oligomer formation is reduced under shading and at higher pH (with use of excess platinum nitrate).

Table 3. The CD and UV Data

Complex	CD $\lambda_{\max}/\text{nm}(\Delta\epsilon)$	UV $\lambda_{\max}/\text{nm}(\epsilon_{\max})$
[Pt( <i>RR</i> -dach)( <i>R</i> -md)]	365(+0.16), 321(+0.19), 253(+2.2), 216(−12)	332(3.8×10 <sup>−3</sup> )
[Pt( <i>RR</i> -dach)( <i>S</i> -md)]	387(−0.09), 326(+0.77), 252(−1.3), 216(+8)	332(4.0×10 <sup>−3</sup> )
[Pt( <i>SS</i> -dach)( <i>R</i> -md)]	386(+0.08), 327(−0.78), 254(+1.2), 216(−11)	332(3.0×10 <sup>−3</sup> )
[Pt( <i>SS</i> -dach)( <i>S</i> -md)]	363(−0.17), 319(−0.21), 254(−2.2), 219(+12)	330(3.7×10 <sup>−3</sup> )
[Pt( <i>RR</i> -dach)(NO <sub>3</sub> ) <sub>2</sub> ]	330(+0.40), 246(+1.03)	—
[Pt( <i>SS</i> -dach)(NO <sub>3</sub> ) <sub>2</sub> ]	330(−0.35), 246(−0.95)	—
[Pt(NH <sub>3</sub> ) <sub>2</sub> ( <i>R</i> -md)]	386(+0.11), 336(−0.31), 255(+1.9)	—
[Pt( <i>ipr</i> ) <sub>2</sub> ( <i>S</i> -md)]	395(−0.11), 340(+0.28), 253(−2.4)	—

**Spectroscopic Properties.** The CD and UV data are listed in Table 3. The CD spectra of [Pt(*RR*-dach)(*R*-md)] and [Pt(*RR*-dach)(*S*-md)] are inverse to those of their enantiomers, [Pt(*SS*-dach)(*S*-md)] and [Pt(*SS*-dach)(*R*-md)], respectively. On the other hand, the spectra of diastereomers are quite different from each other, indicating a marked influence of the mandelate ligands. The additivity rule due to ligand contributions is generally applied to the CD spectra of coordination compounds. The notable contribution of mandelate is rationalized on the assumption that it is bound to platinum(II) by both carboxylato- and alcoholato-oxygens because the chelate configurations have great effects on the CD spectra. If mandelate is linked to the metal via only carboxylato-oxygen, namely in a unidentate fashion, only a vicinal effect could be observed in the CD spectra as a minor contribution. Free mandelic acid has a weak CD at 250 nm or longer wavelength,<sup>20)</sup> which is not consistent with the observed strong CD curve. These CD data suggest mandelate chelation in solution.

The CD spectrum of [Pt(dach)(NO<sub>3</sub>)<sub>2</sub>] has two peaks ( $\lambda_{\max}$  330 and 246 nm) assignable to  $^1A_{1g} \rightarrow ^3E_g$  and  $^1A_{1g} \rightarrow ^1E_g$ , respectively.<sup>21)</sup> Hawkins et al. reported that the octant sign was negative when  $^1A_{1g} \rightarrow ^1E_g$  transition had a positive Cotton effect.<sup>22)</sup> In the case of the square planar complexes, the five-membered chelate with  $\lambda$ -gauche conformation has a negative octant sign. The  $^1A_{1g} \rightarrow ^1E_g$  transition of [Pt(*RR*-dach)(NO<sub>3</sub>)<sub>2</sub>] shows a positive Cotton effect and is assumed to have  $\lambda$ -gauche conformation, which is consistent with the (*1R,2R*)-configuration of the ligand.

The complex [Pt(NH<sub>3</sub>)<sub>2</sub>(*R*-md)] has four donor atoms (i.e., two nitrogen and two oxygen atoms) in common with [Pt(*RR*-dach)(NO<sub>3</sub>)<sub>2</sub>]. It is therefore expected that the CD spectrum of the former complex may have the  $^1A_{1g} \rightarrow ^1E_g$  transition at similar wavelength as that of the latter complex. A  $\lambda_{\max}$  peak at 255 nm, which shows a positive Cotton effect, may be assigned to the  $^1A_{1g} \rightarrow ^1E_g$  transition. In this way we can estimate that the mandelate chelate may have a  $\lambda$ -gauche conformation in aqueous solution. However, this proposal might not be reliable since the mandelate chelate contains a carboxyl group and its symmetry is lower than that of *RR*-dach chelate. In any case, the CD data support the (*R*)-configuration of

the mandelate.

The CD spectra of the four isomers, [Pt(dach)(md)] are essentially linear combinations of those of [Pt(dach)(NO<sub>3</sub>)<sub>2</sub>], [Pt(NH<sub>3</sub>)<sub>2</sub>(*R*-md)], and/or [Pt(*ipr*)<sub>2</sub>(*S*-md)]. This result suggests again that the configurations of the ligands are retained on the coordination to platinum(II).

The <sup>1</sup>H NMR spectra were measured for a pair of diastereomers, [Pt(*RR*-dach)(*S*-md)] and [Pt(*RR*-dach)(*R*-md)]. The dach ligand of [Pt(*RR*-dach)(*S*-md)] shows two sets of multiplets due to the methine protons, since these protons become nonequivalent with the coordination of asymmetric mandelate. In the case of [Pt(*RR*-dach)(*R*-md)], such a separation of methine protons is not observed. Both diastereomers also show the mandelate-methine proton as a singlet; unfortunately, though, the coupling with <sup>195</sup>Pt, the corroborative evidence,<sup>8)</sup> cannot be detected under the influence of too large an HDO signal. Several attempts to reduce the HDO signal (such as a WEFT method, an off-resonance decoupling or the recrystallization from D<sub>2</sub>O) have been unsuccessful up to the present. As a whole, the chemical shifts of both diastereomers bear a close resemblance to each other, but only slight differences have been observed on the phenyl proton signals. These differences may be caused by the mandelate conformations.

The <sup>13</sup>C NMR spectrum was measured for the soluble isomer, [Pt(*SS*-dach)(*R*-md)] in DMSO-*d*<sub>6</sub>. Since the mandelate ligand is asymmetric, splits of 1,2- and 3,6-dach carbons are observed. On the methine carbons of both dach and mandelate, no satellite peaks have been detected, though the observed signals are somewhat broad.

The <sup>195</sup>Pt NMR spectra of both [Pt(*RR*-dach)(*R*-md)] and [Pt(*RR*-dach)(*S*-md)] have a broad peak at ca. −1900 ppm. Usually, the chemical shifts of <sup>195</sup>Pt NMR range very widely from compound to compound. The shift differences between the isomers are negligibly small, in due consideration of the concentration difference in solution. The observed shift-values belong to the range characteristic of a type of coordination compound, PtN<sub>2</sub>O<sub>2</sub>, which consists of the four donor atoms (two nitrogens, two oxygens) and a platinum atom. After 60 days standing in solution, the original compound, [Pt(*RR*-dach)(*S*-

md)], partly changed into another species; a new peak was observed at  $-2970$  ppm. On the other hand, the isomer,  $[\text{Pt}(\text{RR-dach})(\text{R-md})]$ , did not change at all. The half decay time of the original peak was ca. 25 days. The new species is tentatively assignable to a platinum-dimethyl sulfoxide ( $\text{DMSO-}d_6$ ) complex in which dmso is bound to platinum(II) through an S atom, while mandelate coordinates via only carboxylate-oxygen. A similar reaction between dmso and  $\text{cis-}[\text{Pt}(\text{NH}_3)_2\text{Cl}_2]$  was reported,<sup>23)</sup> but the half decay time of the original peak due to cis-platin is 3 h which is much shorter than that of  $[\text{Pt}(\text{RR-dach})(\text{S-md})]$ . From the comparison, it is obvious that the mandelate chelate is relatively stable in solution in spite of the expected instability of platinum alkoxide.

Thus, all CD and NMR results are consistent with the chelate structure of mandelatoplatinum(II) complexes in solution.

The solid state IR spectra of  $[\text{Pt}(\text{RR-dach})(\text{R-md})] \cdot \text{H}_2\text{O}$  and  $[\text{Pt}(\text{RR-dach})(\text{S-md})] \cdot \text{H}_2\text{O}$  are identical to  $[\text{Pt}(\text{SS-dach})(\text{R-md})] \cdot \text{H}_2\text{O}$ , and  $[\text{Pt}(\text{SS-dach})(\text{R-md})] \cdot \text{H}_2\text{O}$ , respectively.

The C=O stretching absorption appears at  $1710\text{ cm}^{-1}$  for mandelic acid<sup>24)</sup> and at  $1582\text{ cm}^{-1}$  for potassium mandelate.<sup>25)</sup> The mandelatoplatinum complexes, i.e., the  $[\text{Pt}(\text{dach})(\text{md})] \cdot \text{H}_2\text{O}$  isomers and  $[\text{Pt}(\text{NH}_3)_2(\text{R-md})] \cdot 1/2\text{H}_2\text{O}$  have the absorption bands between these peaks. As a consequence of the reduced resonance by coordination, the complexes increase the bond strength of C=O in comparison with that of free mandelate. The spectrum of  $[\text{Pt}(\text{RR-dach})(\text{R-md})] \cdot \text{H}_2\text{O}$  shows the C=O stretching at  $1649\text{ cm}^{-1}$  while the band position of  $[\text{Pt}(\text{RR-dach})(\text{S-md})] \cdot \text{H}_2\text{O}$  is  $15\text{ cm}^{-1}$  higher. Such a difference between the diastereomers might be caused by the hydrogen-bonding patterns to a carboxyl oxygen.

**Structure Description of  $[\text{Pt}(\text{dach})(\text{md})] \cdot \text{H}_2\text{O}$  Isomers.** The crystal structure of  $[\text{Pt}(\text{RR-dach})(\text{R-md})] \cdot \text{H}_2\text{O}$  is shown in Fig. 2. Two complexes and two water molecules are crystallographically independent.

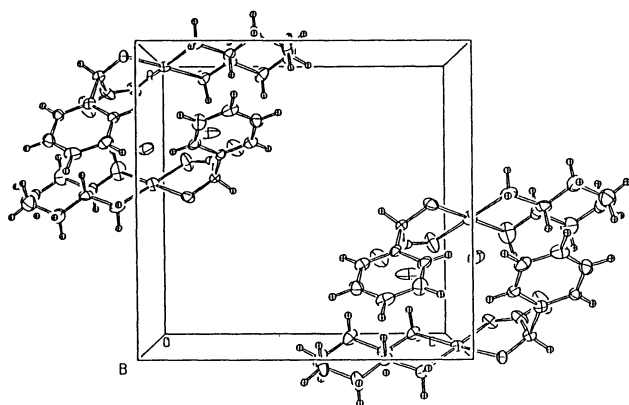


Fig. 2. ORTEP<sup>26)</sup> plot of crystal structure of  $[\text{Pt}(\text{RR-dach})(\text{R-md})] \cdot \text{H}_2\text{O}$ . View along b-axis.

These two complexes form a rather discrete cluster; the two independent complexes are related by a pseudo 2-fold axis. Their coordination planes are approximately perpendicular to each other.

The molecular structure of the complex, i.e., crystallographically independent unit of  $[\text{Pt}(\text{RR-dach})(\text{R-md})] \cdot \text{H}_2\text{O}$ , is shown in Fig. 3. The bond lengths and angles are listed in Table 4. Both ligands, namely *RR-dach* and *R-md*, retain their skeletal configurations. The *RR-dach* has a  $\lambda$ -gauche chelate

Table 4. Bond Lengths (Å) and Angles (°) of  $[\text{Pt}(\text{RR-dach})(\text{R-md})] \cdot \text{H}_2\text{O}$  with e.s.d.'s in Parentheses

Bond length (Å)			
Pt1-O1	2.02(1)	Pt1-O2	2.02(1)
Pt1-N2	2.03(2)	Pt2-O11	1.95(1)
Pt2-N11	2.02(2)	Pt2-N12	1.94(2)
O2-C12	1.43(2)	O3-C11	1.22(2)
O12-C32	1.41(2)	O13-C31	1.23(2)
N2-C2	1.49(2)	N11-C21	1.44(3)
C1-C2	1.53(3)	C1-C6	1.52(3)
C3-C4	1.51(3)	C4-C5	1.57(4)
C11-C12	1.53(3)	C12-C13	1.52(2)
C13-C18	1.36(2)	C14-C15	1.38(2)
C16-C17	1.40(3)	C17-C18	1.37(3)
C21-C26	1.53(3)	C22-C23	1.47(3)
C24-C25	1.47(5)	C25-C26	1.52(3)
C32-C33	1.53(3)	C33-C34	1.40(2)
C34-C35	1.37(2)	C35-C36	1.36(3)
C37-C38	1.38(3)		
Bond angle (°)			
O1-Pt1-O2	83.3(5)	O1-Pt1-N1	95.5(6)
O1-Pt1-N2	178.2(6)	O2-Pt1-N1	178.4(6)
O2-Pt1-N2	97.9(5)	N1-Pt1-N2	82.3(6)
O11-Pt2-O12	82.2(5)	O11-Pt2-N11	98.0(7)
O11-Pt2-N12	178.3(6)	O12-Pt2-N11	178.2(8)
O12-Pt2-N12	99.4(6)	N11-Pt2-N12	80.4(7)
Pt1-O1-C11	114(1)	Pt1-O2-C12	108(1)
Pt2-O11-C31	117(1)	Pt2-O12-C32	109(1)
Pt1-N1-C1	112(1)	Pt1-N2-C2	111(1)
Pt2-N11-C21	111(1)	Pt2-N12-C21	115(1)
N1-C1-C2	112(2)	N1-C1-C6	117(2)
C2-C1-C6	109(2)	N2-C2-C1	106(2)
N2-C2-C3	116(2)	C1-C2-C3	116(2)
C2-C3-C4	111(2)	C3-C4-C5	112(2)
C4-C5-C6	109(2)	C1-C6-C5	113(2)
O1-C11-O3	125(3)	O1-C11-C12	117(2)
O3-C11-C12	118(2)	O2-C12-C11	114(2)
O2-C12-C13	112(2)	C11-C12-C13	108(1)
C12-C13-C14	119(2)	C12-C13-C18	122(2)
C14-C13-C18	119(2)	C13-C14-C15	121(2)
C14-C15-C16	118(2)	C15-C16-C17	120(2)
C16-C17-C18	119(2)	C13-C18-C17	122(2)
N11-C21-C22	107(2)	N11-C21-C26	115(2)
C22-C21-C26	109(2)	N12-C22-C21	101(2)
N12-C22-C23	116(2)	C21-C22-C23	114(2)
C22-C23-C24	110(2)	C23-C24-C25	114(2)
C24-C25-C26	111(2)	C21-C26-C25	112(2)
O11-C31-O13	125(2)	O11-C31-C32	116(2)
O13-C31-C32	119(2)	O12-C32-C31	113(2)
O12-C32-C33	110(2)	C31-C32-C33	112(1)
C32-C33-C34	121(2)	C32-C33-C38	122(2)
C34-C33-C38	117(2)	C33-C34-C35	122(2)
C34-C35-C36	119(2)	C35-C36-C37	120(2)
C36-C37-C38	120(2)	C33-C38-C37	121(2)

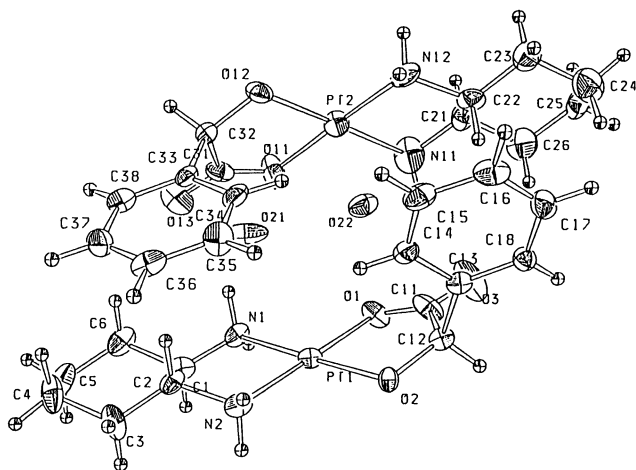


Fig. 3. ORTEP<sup>26</sup>) of molecular structure of  $[\text{Pt}(\text{RR-dach})(\text{R-md})] \cdot \text{H}_2\text{O}$ .

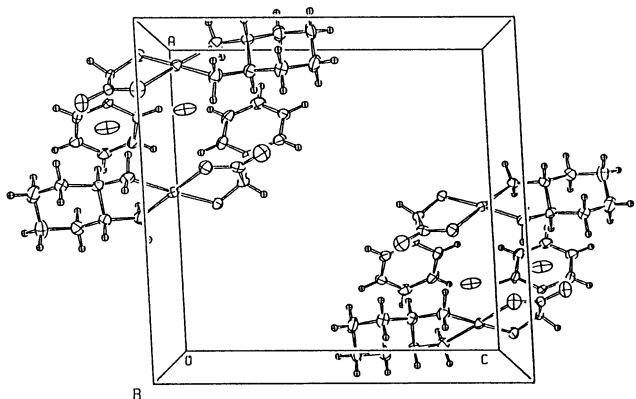


Fig. 4. Crystal structure of  $[\text{Pt}(\text{RR-dach})(\text{S-md})] \cdot \text{H}_2\text{O}$ . View along b-axis.

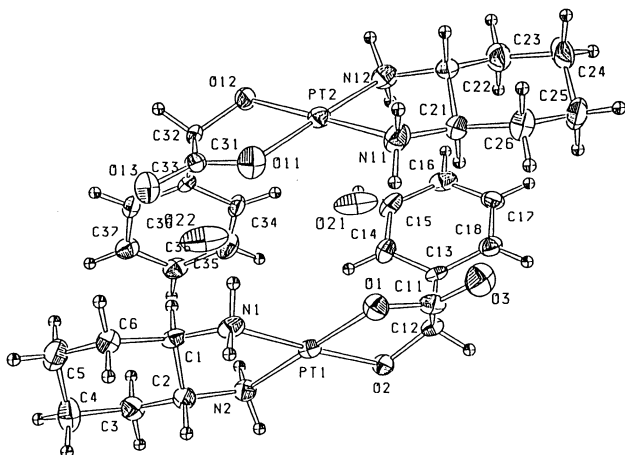


Fig. 5. Molecular structure of  $[\text{Pt}(\text{RR-dach})(\text{S-md})] \cdot \text{H}_2\text{O}$ .

conformation. The mandelate ligand shows bidentate chelation to the platinum atom with carboxylate and alcoholate. Though several mandelate complexes have been reported, their mandelate groups are bound to metals using only carboxylate oxygens.<sup>27,28)</sup>

Table 5. Bond Lengths (Å) and Angles (°) of  $[\text{Pt}(\text{RR-dach})(\text{S-md})] \cdot \text{H}_2\text{O}$  with e.s.d.'s in Parentheses

Bond length (Å)			
Pt1-O1	2.01(1)	Pt1-O2	2.02(1)
Pt1-N2	2.04(1)	Pt2-O11	2.00(1)
Pt2-N11	2.03(2)	Pt2-N12	2.01(2)
O2-C12	1.41(2)	O3-C11	1.20(2)
O12-C32	1.38(2)	O13-C31	1.21(2)
N2-C2	1.48(2)	N11-C21	1.48(2)
C1-C2	1.53(2)	C1-C6	1.53(2)
C3-C4	1.51(3)	C4-C5	1.56(3)
C11-C12	1.53(2)	C12-C13	1.51(2)
C13-C18	1.39(2)	C14-C15	1.38(2)
C16-C17	1.37(3)	C17-C18	1.37(2)
C21-C26	1.52(2)	C22-C23	1.47(3)
C24-C25	1.58(3)	C25-C26	1.52(3)
C32-C33	1.48(2)	C33-C34	1.41(2)
C32-C35	1.39(2)	C35-C36	1.36(3)
C37-C38	1.39(2)		
Bond angle (°)			
O1-Pt1-O2	83.8(5)	O1-Pt1-N1	94.5(5)
O1-Pt1-N2	177.1(6)	O2-Pt1-N1	177.4(5)
O2-Pt1-N2	98.5(5)	N1-Pt1-N2	83.2(6)
O11-Pt2-O12	83.1(5)	O11-Pt2-N11	95.2(6)
O11-Pt2-N12	178.2(6)	O12-Pt2-N11	178.1(6)
O12-Pt2-N12	98.5(6)	N11-Pt2-N12	83.2(6)
Pt1-O1-C11	114(1)	Pt1-O2-C12	109(1)
Pt2-O11-C31	114(1)	Pt2-O12-C32	111(1)
Pt1-N1-C1	109(1)	Pt1-N2-C2	110(1)
Pt2-N11-C21	109(1)	Pt2-N12-C21	111(1)
N1-C1-C2	108(1)	N1-C1-C6	114(1)
C2-C1-C6	110(1)	N2-C2-C1	106(1)
N2-C2-C3	115(1)	C1-C2-C3	111(1)
C2-C3-C4	112(2)	C3-C4-C5	109(2)
C4-C5-C6	112(1)	C1-C6-C5	110(2)
O1-C11-O3	123(2)	O1-C11-C12	115(1)
O3-C11-C12	121(2)	O2-C12-C11	114(1)
O2-C12-C13	113(1)	C11-C12-C13	108(1)
C12-C13-C14	121(1)	C12-C13-C18	121(1)
C14-C13-C18	119(1)	C13-C14-C15	119(2)
C15-C16-C17	120(2)	C15-C16-C17	120(2)
C16-C17-C18	120(2)	C13-C18-C17	121(2)
N11-C21-C22	108(1)	N11-C21-C26	114(2)
C22-C21-C26	111(1)	N12-C22-C21	106(1)
N12-C22-C23	115(2)	C21-C22-C23	113(1)
C22-C23-C24	112(2)	C23-C24-C25	111(1)
C24-C25-C26	110(1)	C21-C26-C25	110(2)
O11-C31-O13	122(2)	O11-C31-C32	116(1)
O13-C31-C32	122(2)	O12-C32-C31	112(1)
O12-C32-C33	113(1)	C31-C32-C33	109(1)
C32-C33-C34	121(1)	C32-C33-C38	122(1)
C34-C33-C38	117(1)	C33-C34-C35	120(2)
C34-C35-C36	122(2)	C35-C36-C37	118(2)
C36-C37-C38	121(2)	C33-C38-C37	121(2)

Thus, the complex,  $[\text{Pt}(\text{RR-dach})(\text{R-md})] \cdot \text{H}_2\text{O}$  is the first example of the bidentate chelate formed by a mandelate ligand. This type of five-membered chelate has been proposed to glycolatoplatinum(II) in solution,<sup>8)</sup> but the solid state structure is unknown to date. For the first time the crystal structure has been firmly determined in this work. Historically, the platinum alkoxides are believed to be unstable<sup>29)</sup> and few examples have been reported so far.<sup>9-11)</sup> In the mandelatoplatinum complex, the metal-alkoxide

Table 6. Possible Hydrogen Bonds ( $\text{\AA}$ )<sup>a)</sup> with e.s.d.'s in Parentheses

[Pt( <i>RR</i> -dach)( <i>R</i> -md)] · H <sub>2</sub> O							
Atom	Atom	Distance	ADC <sup>b)</sup>	Atom	Atom	Distance	ADC
O1	N2	3.20(2)	54702	O2	O21	2.69(2)	55702
O2	N1	3.11(2)	55702	O3	N11	3.12(3)	55501
O11	O21	3.09(2)	55501	O12	O22	2.64(2)	65702
O13	O21	3.06(2)	55501	O21	O22	2.87(3)	55501
O21	N12	2.98(2)	64702	O22	N2	2.87(2)	54702
O22	N11	3.05(2)	55501				
[Pt( <i>RR</i> -dach)( <i>S</i> -md)] · H <sub>2</sub> O							
Atom	Atom	Distance	ADC <sup>b)</sup>	Atom	Atom	Distance	ADC
O1	N2	3.19(2)	65502	O2	O22	2.68(2)	64502
O2	N1	3.14(2)	64502	O11	O22	3.10(2)	55501
O12	O21	2.75(2)	74502	O13	O22	3.06(2)	55501
O21	N2	2.86(2)	65502	O21	O22	2.89(3)	55501
O21	N11	2.99(2)	55501	O22	N12	2.96(2)	55501

a) Intermolecular distances between O and N which are shorter than 3.20 $\text{\AA}$  are listed. b) The atom designator code. The 5-digit number is a composite of three one digit numbers and one two digit number: TA(1st)+TB(2nd)+TC(3rd)+SN(4th and 5th). TA, TB, and TC are the lattice translation along cell edges a, b and c, where digit of 5 indicates the origin cell. The SN is symmetry operation.

Symmetry operators: (1)  $x, y, z$ . (2)  $-x, 1/2+y, -z$ .

bond may be stabilized by five-membered chelation. The phenyl group of mandelate rises up to the axial direction to the coordination plane. Such a direction possibly resulted from the crystal packing. Consequently, the *R*-md has  $\delta$ -gauche conformation in the solid state though  $\lambda$ -gauche conformation is suggested in the aqueous solution by the CD spectra.

The crystal and molecular structures of [Pt(*RR*-dach)(*S*-md)] · H<sub>2</sub>O are depicted in Figs. 4 and 5, respectively. The bond lengths and angles are listed in Table 5. The structural feature is analogous to that of [Pt(*RR*-dach)(*R*-md)] · H<sub>2</sub>O. Two complexes and two water molecules also have crystallographic independence. The configurations of the ligands are retained in comparison with the corresponding free amine or acid. The *RR*-dach ligand has a  $\lambda$ -gauche conformation. The md ligand is bound to the platinum atom to form a five-membered chelate of  $\lambda$ -gauche conformation. The phenyl group rises up to the axial direction to the coordination plane.

Both isomers have a typical square-planar coordination, except for rather small N-Pt-N and O-Pt-O angles due to the five-membered chelation. As a whole, the structural features of both diastereomers (bond lengths and angles) are very similar.

The hydrogen bonds are listed in Table 6. Between the alcoholates and the water molecules, strong hydrogen bonds are formed. The hydrogen-bonding patterns of both isomers have many similarities to each other, though the hydrogen-bond distributions in a pair of diastereomers are slightly different. Fig. 6 shows that only [Pt(*RR*-dach)(*R*-md)] · H<sub>2</sub>O has a hydrogen-bond between carboxylate oxygen and amine nitrogen, directly reflecting the configurations of the two diastereomers. Not only the IR spectra,

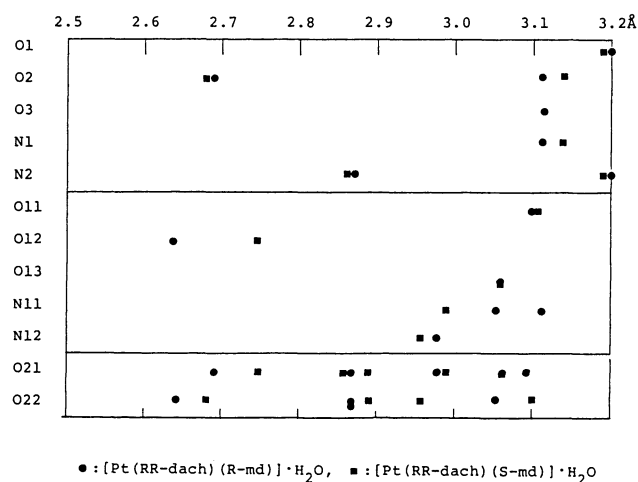


Fig. 6. Hydrogen-bond distributions of two isomers.

but also the solubilities of the diastereomers are practically different from each other. The complex [Pt(*RR*-dach)(*S*-md)] · H<sub>2</sub>O is a more soluble isomer in water or dmso (see Experimental). These experimental facts agree well with the above difference in the hydrogen-bond distributions.

**Antitumor Activities of [Pt(dach)(md)] Isomers.** The results of animal tests against mice leukemia L1210 are listed in Table 7. The complexes show antitumor activities to a certain extent, but not completely. On the other hand, the toxicities are greatly reduced, compared to cis-platin. The four optical isomers exhibit differences in antitumor activities. Complex [Pt(*RR*-dach)(*R*-md)] is effective over a wide range of dose where its enantiomer, [Pt(*SS*-dach)(*S*-md)], shows no activity. The antitumor activity of [Pt(*RR*-dach)(*S*-md)] is similar to that of [Pt(*SS*-

Table 7. Antitumor Activities against Mice Leukemia L1210

Isomer	T/C (%)					
	Dose (mg/kg)					
	400	200	100	50	25	12.5
RR-R	Toxic	126 P	190 P	162 P	137 P	109
RR-S	138 P	160 P	132 P			
SS-R	126 P	156 P	108			
SS-S	Toxic	124	114			

T/C value over 125 was evaluated as antitumor active and indicated with P.

dach)(R-md)], but the toxic dose is different.

These results show that the chiralities of not only the carrier ligands, but that the leaving groups influence the antitumor activities of the complexes. It is also likely that the solubilities of the complexes influence the activities.

## References

- 1) B. Rosenberg, L. Van Camp, J. E. Trosko, and V. H. Mansour, *Nature (London)*, **222**, 385 (1969).
- 2) M. J. Cleare and J. D. Hoeschele, *Bioinorg. Chem.*, **2**, 187 (1973).
- 3) T. A. Connors, M. Jones, W. C. J. Ross, T. D. Braddock, A. R. Khokhar, and M. L. Tobe, *Chem. Biol. Interact.*, **5**, 415 (1972).
- 4) G. R. Gale, E. M. Walker, Jr., L. M. Atkins, A. B. Smith, and S. J. Meischen, *Res. Commun. Chem. Pathol. Pharmacol.*, **7**, 529 (1974).
- 5) Y. Kidani, M. Noji, and T. Tashiro, *Gann*, **71**, 637 (1980).
- 6) K. Maeda, T. K. Miyamoto, Y. Sasaki, and T. Tashiro, *Inorg. Chim. Acta*, **153**, 137 (1988).
- 7) K. Okude, H. Ichida, T. K. Miyamoto, Y. Sasaki, and T. Tashiro, *Chem. Lett.*, **1989**, 119.
- 8) T. Totani, K. Aono, M. Komura, and Y. Adachi, *Chem. Lett.*, **1986**, 429.
- 9) L. S. Hollis, A. R. Amunsen, and E. W. Stern, *J. Am. Chem. Soc.*, **107**, 274 (1985).
- 10) N. W. Alcock, A. W. G. Platt, and P. G. Pringle, *Inorg. Chim. Acta*, **128**, 215 (1987).
- 11) C. D. Montgomery, N. C. Payne, and C. J. Willis, *Inorg. Chem.*, **26**, 519 (1987).
- 12) F. Galsbøl, P. Steenbøl, and B. S. Sørensen, *Acta Chem. Scand.*, **26**, 3605 (1972).
- 13) B. Lippert, C. J. L. Lock, B. Rosenberg, and M. Zvagulis, *Inorg. Chem.*, **16**, 1525 (1977).
- 14) G. J. Gilmore, Mithril: A Computer Program for the Automatic Solution of Crystal Structure from X-ray Data, Univ. of Glasgow, Scotland (1983).
- 15) P. N. Swepston, TEXSAN Software, Molecular Structure Corporation, College Station, Texas, USA (1986).
- 16) International Tables for X-ray Crystallography Vol. IV., Kynoch Press, Birmingham (Present distributor Kluwer Academic Publishers, Dordrecht.) (1974).
- 17) E. Lippert, *ACS Symp. Ser.*, **209**, 147 (1983).
- 18) L. S. Hollis and S. J. Lippard, *J. Am. Chem. Soc.*, **105**, 3494 (1983).
- 19) T. G. Appleton, R. D. Berry, C. A. Davis, J. R. Hall, and H. A. Kilin, *Inorg. Chem.*, **23**, 3514 (1984).
- 20) R. Hakansson and S. Gronowitz, *Tetrahedron*, **32**, 2973 (1976).
- 21) M. Noji, K. Okamoto, Y. Kidani, and T. Tashiro, *J. Med. Chem.*, **24**, 508 (1981).
- 22) C. J. Hawkins and E. Larsen, *Acta Chem. Scand.*, **19**, 185 (1965).
- 23) W. I. Sundquist, K. A. Ahmed, L. S. Hollis, and S. J. Lippard, *Inorg. Chem.*, **26**, 1524 (1987).
- 24) "The Aldrich Library of Infrared Spectra III," ed. by C. J. Pouchert, Aldrich Chemical Company, Milwaukee (1981).
- 25) "The Sadtler Standard Spectra," Vol. 7, No. 6205.
- 26) C. K. Johnson, ORTEP II. Report ORNL-5138. Oak Ridge National Laboratory, Tennessee, USA (1976).
- 27) F. A. Cotton, L. R. Falvello, and C. A. Murillo, *Inorg. Chem.*, **22**, 382 (1983).
- 28) P. A. Agaskar, F. A. Cotton, L. R. Falvello, and S. Han, *J. Am. Chem. Soc.*, **108**, 1214 (1986).
- 29) F. R. Hartley, "The Chemistry of Platinum and Palladium," Applied Science Publishers Ltd., London (1973), Chap. 8.